A non-conserved histidine residue on KRAS drives paralog selectivity of the KRAS^{G12D} inhibitor MRTX1133

Miles A. Keats [1,*], John J. W. Han [1,*], Yeon-Hwa Lee [1], Chih-Shia Lee [1,#] and Ji Luo [1,#]

[1.] Laboratory of Cancer Biology and Genetics, Center for Cancer Research, National Cancer Institute, National Institutes of Health, Bethesda, Maryland, USA

* Equal contribution

[#] Correspondence: chih-shia.lee@nih.gov, ji.luo@nih.gov

Chih-Shia Lee:

Address: 37 Convent Dr., Room 4050, Bethesda, MD 20892

Email: chih-shia.lee@nih.gov

Phone: 240-760-6926

Ji Luo:

Address: 37 Convent Dr., Room 4054B, Bethesda, MD 20892

Email: ji.luo@nih.gov

Phone: 301-451-4725

Running title: Paralog selectivity of the KRAS^{G12D} inhibitor MRTX1133

Conflict of interest disclosure statement: The authors declare no conflict of interest.

SUPPLEMENTARY INFORMATION

SUPPLEMENTARY DISCUSSION

Our analysis of the prototypical $KRAS^{G12D}$ inhibitor MRTX1133 led to several insights that have important implications for the future development of non-covalent KRAS inhibitors. We showed that the D12 mutant residue is important, but not essential, for the activity of MRTX1133. Using isogenic Rasless MEFs that express a single Ras allele, we showed that MRTX1133 can effectively inhibit WT KRAS activity in intact cells, at an IC_{50} that is 4-fold higher than that of KRASG12D. This is unexpected, but not entirely surprising, as MRTX1133 can bind KRAS WT protein in cell-free assays(1). To gain sufficient affinity without the advantage of crosslinking, the MRTX1133 scaffold was extensively optimized for binding to the KRAS switch II pocket. A recent *in silico* binding energy simulation study suggested that the D12 residue, through its interaction with the bicyclic piperazine ring in MRTX1133, contributes approximately -1 kcal/mol out of a total -73 kcal/mol free binding energy for MRTX1133(2). Thus, losing the interaction between the MRTX1133 piperazine ring with D12 seems to reduce, but not abolish, ligand binding. This explains the partial activity of MRTX1133 towards other KRAS mutants including G12C and G13D. The activity of MRTX1133 towards KRAS WT protein could also be attributed to its preference for the GDP-bound form of KRAS. Although MRTX1133 can bind to both GDP- and GTP-bound KRAS in biochemical assays, it binds to the former with substantially higher affinity(1). In cells, KRAS WT protein cycles to the GDP-bound state more rapidly due to the activity of GTPase-activating proteins, making it more readily inhibitable by MRTX1133. This could explain the smaller than expected difference in IC_{50} values (70 nM vs. 296 nM) between KRASG12D and KRAS WT Rasless MEFs. In support of this notion, we noted that the sensitive mutant alleles G12D, G13D, and G12C all have been shown to have higher intrinsic GTPase

activity, whereas the insensitive mutant alleles G12R, Q61R and Q61L have been shown to have low intrinsic GTPase activity(3). The Q61 residue does not make direct interaction with MRTX1133 in the crystal structure. It is possible that mutation at Q61 disrupts MRTX1133 binding, although it is also plausible that MRTX1133 is less effective at inhibiting GTP-bound KRAS in intact cells.

We showed that MRTX1133 exhibits exquisite selectivity for KRAS over its two closely related paralogs HRAS and NRAS. Unlikely G12D and WT forms of KRAS, MRTX1133 was unable to inhibit G12D and WT forms of HRAS and NRAS. Our reciprocal mutation experiments demonstrated that this is entirely due to the non-conserved H95 residue in KRAS that plays a critical role in ligand binding. H95, together with Y64 and Y96 that are coordinated by it, are estimated to contribute approximately -6.6 kcal/mol of free binding energy(2). Q95 and L95 in HRAS and NRAS, respectively, are likely to disrupt this network of interactions and therefore abrogate MRTX1133 binding. The selectivity of MRTX1133 for $KRAS^{G12D}$ over KRAS WT protein, coupled with its ability to fully spare HRAS and NRAS, will likely give it a wide therapeutic window in clinical studies. The KRAS G12C inhibitor sotorasib has a distinct scaffold compared to adagrasib and MRTX1133. In the co-crystal structure of sotorasib covalently bound to $KRAS^{G12C}$, H95 does not directly interact with sotorasib, and all residues that interact with sotorasib are fully conserved across the three Ras paralogs(4). Thus, it is reasonable to postulate that a $KRAS^{G12D}$ inhibitor based on the sotorasib scaffold might also inhibit $HRAS^{G12D}$ and $NRAS^{G12D}$ and thus lack paralog selectivity. Similarly, the covalent $KRAS^{G12C}$ inhibitor JDQ443 des not interact with H95 on KRAS(5). Thus, a $KRAS^{G12D}$ inhibitor based on the JDQ443 scaffold might inhibit $HRAS^{G12D}$ and $NRAS^{G12D}$ as well.

In addition to MRTX1133, several $KRAS^{G12D}$ inhibitors have been developed recently, including ASP3082, HRS-4642 and RMC-9805. However, unlike MRTX1133, the chemical structures of these inhibitors, as well as their co-crystal structures with $KRAS^{G12D}$, are not publicly available at the moment. It is therefore difficult to assess their $KRAS^{G12D}$ selectivity or their paralog selectivity. Furthermore, efforts have also been directed at developing pan-KRAS inhibitors. One example is RMC-6236 that have broader spectrum of activity towards multiple KRAS mutant(6). Currently it is unclear whether RMC-6236 possesses any paralog selectivity. While this manuscript was under review, two pan-KRAS inhibitors were disclosed, BI-2865 and BI-2493. Similar to MRTX1133, BI-2865 exhibit exquisite selectivity for KRAS over HRAS and NRAS. Structural and mutational analysis indicated that H95 was also a critical KRAS-selectivity handle for BI-2865(7). What is salient from our study is that the Rasless MEF system developed by the NCI Ras Initiative, which enables the isolated expression of a single Ras allele in an isogenic background to drive MAPK signaling and cell proliferation, is ideally suited to verify the selectivity of Ras inhibitors. We recommend this system to be routinely used to test the mutant and paralog selectivity of future Ras inhibitors.

Our results, together with the recent work on BI-2865(7), suggest that paralog-selective "pan-KRAS" inhibitors could be developed by exploiting the $KRAS^{H95}$ selectivity handle. Given the critical role of physiological Ras signaling, a pan-Ras inhibitor that does not discriminate among the three Ras paralogs is likely to have significant on-target toxicity as Ras signaling is required to sustain the normal proliferation and turnover of tissues such as the bone marrow and the intestinal epithelium. Because the three Ras paralogs are often co-expressed, a pan-KRAS inhibitor that spares HRAS and NRAS, on the other hand, could be selectively toxic to

KRAS dependent cancer cells while being tolerated in normal tissues(8). Thus, a $KRAS^{G12D}$ inhibitor or a pan-KRAS inhibitor that does not exhibit paralog selectivity might be less tolerated. Our characterization of the selectivity profile of MRTX1133 indicates that binding to a mutant residue, while highly desirable, may not be necessary. BI-2865 demonstrated that it might be possible to develop a chemically related scaffold that preserves binding to H95 but does not extend interaction towards the G12 or G13 position on KRAS(7). Conversely, altering the scaffold such that it specifically interacts with Q95 or L95 but not with H95 could aid the development of HRAS and NRAS paralog-selective inhibitors, respectively, to selectively target HRAS and NRAS mutant tumors.

Lastly, our study suggests a resistance mechanism to MRTX1133. Our data showed that H95 and Y96 are critical for the binding of MRTX1133 to KRAS, and mutation of these residues abrogate sensitivity to MRTX1133. This is analogous to acquired resistance to adagrasib(9,10). We therefore anticipate that secondary mutation at H95 and Y96 will likely be a significant mechanism of acquired resistance to MRTX1133 in clinical studies.

SUPPLEMENTARY REFERENCES

1. Hallin J, Bowcut V, Calinisan A, Briere DM, Hargis L, Engstrom LD*, et al.* Anti-tumor efficacy of a potent and selective non-covalent KRAS(G12D) inhibitor. Nat Med **2022**;28:2171-82
2. Issahaku AR, Mukelabai N, Agoni C, Rudrapal M, Aldosari SM, Almalki SG*, et al.* Characterization of the binding of MRTX1133 as an avenue for the discovery of potential KRAS(G12D) inhibitors for cancer therapy. Sci Rep **2022**;12:17796
3. Hunter JC, Manandhar A, Carrasco MA, Gurbani D, Gondi S, Westover KD. Biochemical and Structural Analysis of Common Cancer-Associated KRAS Mutations. Mol Cancer Res **2015**;13:1325-35
4. Canon J, Rex K, Saiki AY, Mohr C, Cooke K, Bagal D*, et al.* The clinical KRAS(G12C) inhibitor AMG 510 drives anti-tumour immunity. Nature **2019**;575:217-23
5. Lorthiois E, Gerspacher M, Beyer KS, Vaupel A, Leblanc C, Stringer R*, et al.* JDQ443, a Structurally Novel, Pyrazole-Based, Covalent Inhibitor of KRAS(G12C) for the Treatment of Solid Tumors. J Med Chem **2022**;65:16173-203
6. Mullard A. The KRAS crowd targets its next cancer mutations. Nat Rev Drug Discov **2023**;22:167-71
7. Kim D, Herdeis L, Rudolph D, Zhao Y, Bottcher J, Vides A*, et al.* Pan-KRAS inhibitor disables oncogenic signalling and tumour growth. Nature **2023**
8. Hofmann MH, Gerlach D, Misale S, Petronczki M, Kraut N. Expanding the Reach of Precision Oncology by Drugging All KRAS Mutants. Cancer Discov **2022**;12:924-37
9. Tanaka N, Lin JJ, Li C, Ryan MB, Zhang J, Kiedrowski LA*, et al.* Clinical acquired resistance to KRASG12C inhibition through a novel KRAS switch-II pocket mutation and polyclonal alterations converging on RAS-MAPK reactivation. Cancer Discov **2021**
10. Awad MM, Liu S, Rybkin, II, Arbour KC, Dilly J, Zhu VW*, et al.* Acquired Resistance to KRAS(G12C) Inhibition in Cancer. N Engl J Med **2021**;384:2382-93

SUPPLEMENTARY TABLES

Supplementary Table 1. Cell line authentication and mycoplasma test information

Cell lines	Authentication dates	Mycoplasma testing dates
A549	6/11/2015, 5/5/2023	4/10/2023
AsPC-1	5/5/2023	4/10/2023
H358 (NCI-H358)	2/2/2021, 5/5/0203	9/29/2021, 4/10/2023
H2030 (NCI-H2030)	6/11/2015, 2/2/2021, 5/5/2023	4/10/2023
HT-29	2/18/2022, 5/5/2023	10/28/2020
INA-6	9/5/2020	1/20/2022
KP-4	5/5/2023	4/14/2023, 4/25/2023, 5/11/2023
Panc10.05	9/29/2021, 5/5/2023	9/29/2023, 4/10/2023
SW620	6/11/2015, 5/5/2023	4/10/2023
SW1990	2/18/2022, 5/5/2023	4/14/2023, 4/25/2023, 5/11/2023

Supplementary Table 2. Antibodies for immunoblotting

Target	Manufacturer	Catalog number	Dilution
Ras (pan)	Sigma-Aldrich	OP40	1:1,000
KRAS	Sigma-Aldrich	WH0003845M1	1:250
p-ERK1/2	Cell Signaling Technology	4377	1:1,000
ERK1/2	Cell Signaling Technology	9102	1:1,000
Vinculin	Santa Cruz Biotechnology	SC-25336	1:1,000
GAPDH	Santa Cruz Biotechnology	SC-365062	1:5,000
Mouse IgG	Jackson ImmunoResearch	115-036-072	1:5,000
Rabbit IgG	Jackson ImmunoResearch	111-036-047	1:5,000

Supplementary Table 3. Site-directed mutagenesis primers

Human Ras cDNA	Desired mutation	Forward primer sequence (5' to 3')	Reverse primer sequence (5' to 3')
KRAS4B	H95Q	ATAATACTAAATCATTTGAAGATATTCACCAATATAGAGAACAAATTAAAAGAGTTAAGG	CCTTAACTCTTTTAATTTGTTCTCTATATTGGTGAATATCTTCAAATGATTTAGTATTAT
KRAS4B	H95L	TAATACTAAATCATTTGAAGATATTCACCTTTATAGAGAACAAATTAAAAGAGTTAAGG	CCTTAACTCTTTTAATTTGTTCTCTATAAAGGTGAATATCTTCAAATGATTTAGTATTA
KRAS4B	Y96D	ATAATACTAAATCATTTGAAGATATTCACCATGATAGAGAACAAATTAAAAGAGTTAAGG	ATAATACTAAATCATTTGAAGATATTCACCATGATAGAGAACAAATTAAAAGAGTTAAGG
HRAS	Q95H	CTTTTGAGGACATCCACCATTACAGGGAGCAGATCAAAC	GTTTGATCTGCTCCCTGTAATGGTGGATGTCCTCAAAAG
NRAS	L95H	GTCATTTGCGGATATTAACCACTACAGGGAGCAGATTAAGCG	CGCTTAATCTGCTCCCTGTAGTGGTTAATATCCGCAAATGAC

Supplementary Table 4. Primers for PCR-cloning HA-Ras into pLVX-Puro vector

Human Ras cDNA	Forward primer sequence (5' to 3')	Reverse primer sequence (5' to 3')
KRAS4B	GGCGGCCGCACCATGTACCCATACGATGTTCCAGATTACGCTGGAGGATCAGGAACTGAATATAAACTTGTGGTAGTTG	GGAGGGATCCTTACATAATTACACACTTTGTCTTTG
HRAS	GGCGGCCGCACCATGTACCCATACGATGTTCCAGATTACGCTGGAGGATCAGGAACGGAATATAAGCTGGTGGTGG	GGAGGGATCCTTAGGAGAGCACACACTTGCAGC
NRAS	GGCGGCCGCACCATGTACCCATACGATGTTCCAGATTACGCTGGAGGATCAGGAACTGAGTACAAACTGGTGGTGGTTGG	GAGGGATCCTTACATCACCACACATGGCAATCCC

SUPPLEMENTARY FIGURE LEGENDS

Supplementary Figure S1. INA6 cells are dependent on NRAS.

DepMap database *NRAS* gene dependency score (DepMap Public 22Q4+Score, Chronos) for human multiple myeloma cell lines harboring *NRAS* mutation. CRISPR/Cas9-mediated gene knockout effect was from the DepMap data portal (https://depmap.org/portal/). A negative score indicates the cell line is sensitive to knocking out the indicated gene and therefore is dependent on the gene for viability.

Supplementary Figure S2. The non-conserved histidine 95 on KRAS makes critical contribution to MRTX1133 ligand binding.

A. Amino acid sequence alignment of human KRAS4B^{G12D}, WT HRAS, and WT NRAS. The P-loop, Switch I and Switch II domains, and the hypervariable region are labeled. Amino acid residues of KRAS^{G12D} that interact with MRTX1133 are colored in red. Residues that are conserved among the three Ras sequences are colored in grey, while the residues that are not conserved are bold and colored in black. Among all the MRTX1133-interacting residues in KRAS^{G12D}, only H95 (red arrow) is not conserved in HRAS and NRAS.

B. Interactions of MRTX1133 with H95 on KRAS^{G12D}. Top panel, structure of the MRTX1133 binding pocket in KRAS^{G12D} in the GDP-bound form illustrating the role H95 plays in stabilizing ligand binding (PDB: 7RPZ). Bottom panel, a schematic view of the interactions between MRTX1133 and Y64, H95, and Y96 residues of KRAS.

C. Experimental design for testing the hypothesis that H95 on KRAS provides a critical selectivity handle for MRTX1133. Different HA-tagged Ras double mutants were transduced into KRAS^{G12D} Rasless MEFs to test how they alter the cells' sensitivity to MRTX1133.

D. A schematic view of the interactions between adagrasib and Y64, H95, and Y96 residues of KRAS (based on PDB: 6UT0).

Supplementary Figure S3. Mutation in H95 and Y96 on KRAS as a potential mechanism for acquired resistance to MRTX1133.

A-B. Human pancreatic cancer cell line KP4 (**A**) and SW1990 (**B**) were stably transduced with HA-tagged KRAS mutants as indicated. Cells were treated with MRTX1133 for 3 days and cell viability was determined using CellTiter-Glo assay. Dose-response curves were fitted from three to four independent repeats (error bars represent S.D.)

C-D. Cells used in panel **A** and **B** were treated with or without 1 μM MRTX1133 (+) or DMSO (-) for one day. Cell lysates were harvested and immunoblotted for pERK and total ERK (a representative of two independent experiments is shown).

Supplementary Figure S1.

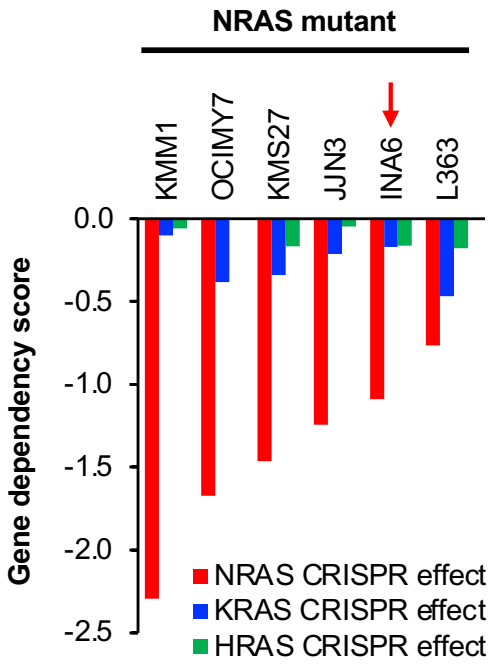

Supplementary Figure S2.

A

```
                    10        20        30        40        50
                    |         |         |         |         |
KRAS4B_G12D  MTEYKLVVVGADGVGKSALTIQLIQNHFVDEYDPTIEDSYRKQVVIDGET 50
HRAS_WT      MTEYKLVVVGAGGVGKSALTIQLIQNHFVDEYDPTIEDSYRKQVVIDGET 50
NRAS_WT      MTEYKLVVVGAGGVGKSALTIQLIQNHFVDEYDPTIEDSYRKQVVIDGET 50
                    [P-loop]          [Switch I]

                    60        70        80        90        100
                    |         |         |         |         |
KRAS4B_G12D  CLLDILDTAGQEEYSAMRDQYMRTGEGFLCVFAINNTKSFEDIHHYREQI 100
HRAS_WT      CLLDILDTAGQEEYSAMRDQYMRTGEGFLCVFAINNTKSFEDIHQYREQI 100
NRAS_WT      CLLDILDTAGQEEYSAMRDQYMRTGEGFLCVFAINNSKSFADINLYREQI 100
                    [Switch II]

                    110       120       130       140       150
                    |         |         |         |         |
KRAS4B_G12D  KRVKDSEDVPMVLVGNKCDLPSRTVDTKQAQDLARSYGIPFIETSAKTRQ 150
HRAS_WT      KRVKDSDDVPMVLVGNKCDLAARTVESRQAQDLARSYGIPYIETSAKTRQ 150
NRAS_WT      KRVKDSDDVPMVLVGNKCDLPTRTVDTKQAHELAKSYGIPFIETSAKTRQ 150

                    160       170       178/180   188/189
                    |         |         |         |
KRAS4B_G12D  GVDDAFYTLVREIRKHKEKM-SKD-GKKKKKKSKTKCVIM 188
HRAS_WT      GVEDAFYTLVREIRQHKLRKLNPPDESGPGCMSCK-CVLS 189
NRAS_WT      GVEDAFYTLVREIRQYRMKKLNSSDDGTQGCMGLP-CVVM 189
                                [Hypervariable region]
```

Color key:
Gray: conserved residues
Black: non-conserved residues
Red: residues in contact with MRTX1133

B

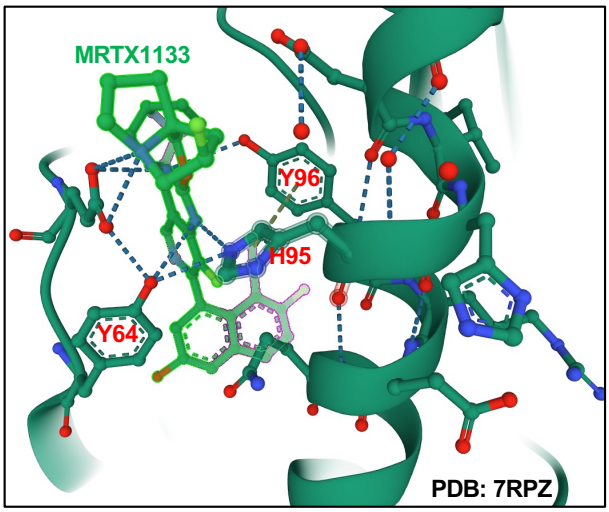

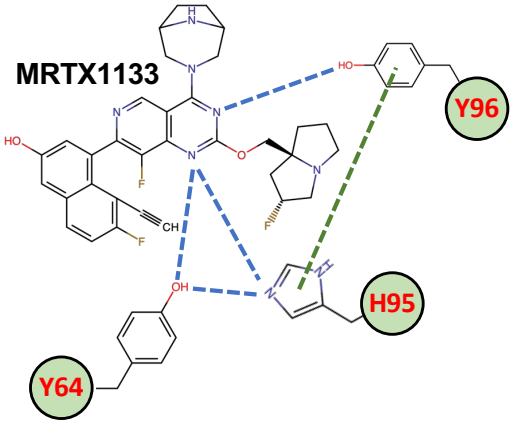

C

Predicted MRTX1133 sensitivity	Mutant cDNA tested
+	HA-KRAS G12D
–	HA-KRAS G12D/H95Q
–	HA-KRAS G12D/H95L
–	HA-HRAS G12D
+	HA-HRAS G12D/Q95H
–	HA-NRAS G12D
+	HA-NRAS G12D/L95H
–	HA-KRAS G12D/Y96D

→ KRAS G12D RASless MEFs →

Assay readout

Cell viability
Active Ras level
pERK level

D

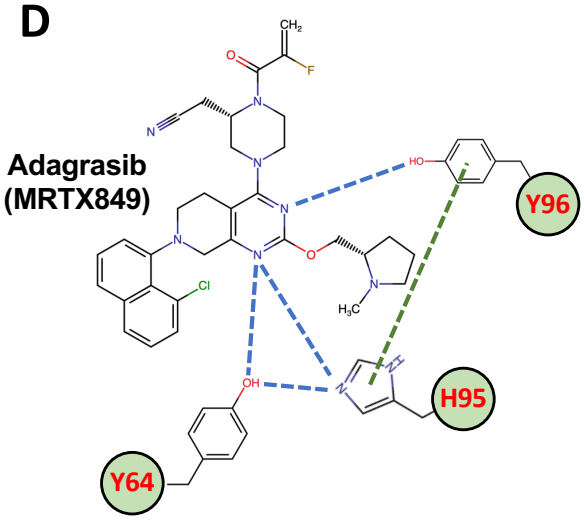

Supplementary Figure S3.